

# Markov Model of Terrain for Evaluation of Ground Proximity Warning System Thresholds

James K. Kuchar\*

*Massachusetts Institute of Technology, Cambridge, Massachusetts 02139*

**A statistical model of terrain was developed to estimate the probability of a controlled flight into terrain accident following a ground proximity warning system (GPWS) alert. The terrain model was derived from an actual terrain database and used to create a Markov chain simulation. With this simulation the probability of terrain impact was computed as a function of terrain type and aircraft trajectory profile. Contours of collision probability were then generated and plotted against current alerting thresholds, illustrating how threshold placement maps into safety. Example results for the GPWS excessive descent rate alerting mode are provided. Following a warning and the subsequent pilot reaction delay and pull-up maneuver, the probability of collision with relatively flat terrain is less than  $1 \times 10^{-8}$  for high descent rates. In steep, rapidly changing terrain, the probability of collision following an alert increases to more than 0.01. A simple modification of alerting thresholds would not resolve this problem because of a resulting higher rate of nuisance alarms, as shown quantitatively by a performance tradeoff curve. Potential performance improvements through decreased response time or increased maneuvering load factor are also quantified.**

## I. Introduction

THE Ground Proximity Warning System (GPWS) provides an alert to civil transport flight crews when the aircraft is in danger of impacting terrain. GPWS was mandated on jet transports in the United States following several controlled flight into terrain (CFIT) accidents, notably the crash of a Trans World Airlines Boeing 727 into hills west of Dulles International Airport on 1 December, 1974.<sup>1,2</sup> Since its introduction, GPWS has played a major part in reducing CFIT accidents, defined as cases in which an aircraft in controllable and sustainable flight collides with terrain. However, CFIT accidents still occur, even on aircraft with functioning GPWS equipment, and CFIT remains a major category of aviation fatalities.

Approximately 35% of the CFIT accidents between 1975 and 1992 involved aircraft with a functioning GPWS.<sup>3</sup> On aircraft that had a working GPWS system, CFIT accidents occurred in one of three categories:

1) No warning of impending impact was given in 24% of CFIT accidents with a functioning GPWS system. These cases generally involved an aircraft descending while in landing configuration (i.e., landing gear is down, and flaps are extended). Because false alarms are undesirable during final approach to an airport, GPWS is designed to become less sensitive to terrain hazards when the aircraft is in the landing configuration.

2) Late warnings, in which the pilot had too little time to respond to an alert, contributed to 38% of the CFIT accidents with a functioning GPWS system. To prevent an excessive number of false alarms, the alerting thresholds are set such that alerts may be late if terrain rises extremely rapidly.

3) Poor pilot response was found to contribute to 38% of the CFIT accidents with a functioning GPWS system. In these cases GPWS provided adequate time to react to a hazard, but the crew delayed their response or made an inadequate avoidance maneuver. In some cases the delayed response has been attributed to previously experienced false alarms with GPWS.<sup>4</sup>

GPWSs currently in place on transport aircraft rely upon both barometric and radar altitude measurements to determine if an alert needs to be issued. The barometric altimeter measures altitude above mean sea level (MSL) and does not by itself provide a measure of

altitude above terrain. The radar altimeter provides a measurement of the above ground level (AGL) altitude of the aircraft. AGL altitude is calculated from the time delay in a radar pulse beamed at the ground below the aircraft. The rate of change in MSL altitude or AGL altitude is then extrapolated to estimate the danger posed by proximity to terrain. Because of its beamwidth, the existence of side lobes, and changes in orientation caused by aircraft pitch and roll, the radar altimeter does not always indicate the actual altitude over the terrain directly below the aircraft.

The primary shortcoming of GPWS is that limited information is available to the system regarding the terrain ahead or to the side of the flight path. The system must, in effect, extrapolate the terrain altitude ahead of the aircraft based on the current altitude rate measurements. Because of this limitation, false alarms may occur when flying over small, sheer terrain rises because the extrapolated terrain slope appears to be hazardous. Missed detections are also possible when flying into rapidly rising terrain if the terrain slope is underestimated. To be effective, GPWS alerting logic must attempt to minimize both of these effects.

Improvements in terrain proximity alerting are possible through the use of an onboard terrain database. Terrain referenced navigation (TRN) and guidance systems have been under development for over a decade.<sup>5–10</sup> In addition to providing improved navigation and guidance capabilities, correlating the aircraft position with terrain data enhances the ability to accurately predict terrain hazards and perform terrain avoidance (TA).<sup>6–8</sup> Also, the use of a terrain database enables the display of the terrain field to the pilot, improving situation awareness, and providing corroborating information when an alert is issued.<sup>11</sup> Although much of the work in TRN and TA has been for military applications (such as low-level terrain following), civil transport alerting systems based on terrain databases are also being fielded.<sup>12</sup>

Terrain-database-enhanced navigation, guidance, and warning systems are likely to be significant players in further improving aviation safety. This paper, however, focuses on the design of the underlying radar-based GPWS alerting thresholds, which continue to fill a role as the final safety net before CFIT accidents occur.

## II. GPWS Operation

GPWS systems on U.S. jet transport aircraft must comply with a series of performance specifications, designed to protect against a variety of CFIT accident types.<sup>2,13</sup> The examples here, however, concern only those situations in which the aircraft is descending toward a terrain field while not in landing configuration (i.e., landing gear is up, and flaps are retracted).

Received 23 March 2000. Copyright © 2001 by James K. Kuchar. Published by the American Institute of Aeronautics and Astronautics, Inc., with permission.

\*Associate Professor of Aeronautics and Astronautics, Room 33-305, 77 Massachusetts Avenue; jkkuchar@mit.edu. Member AIAA.

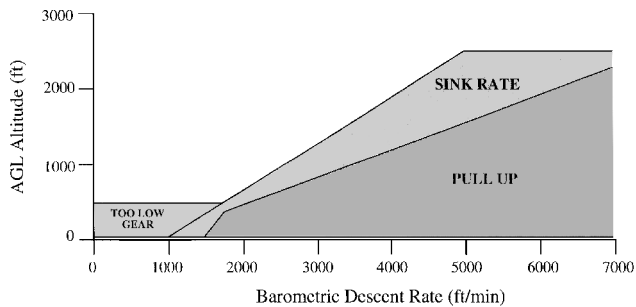


Fig. 1 GPWS alerting thresholds (excessive descent rate mode).<sup>14</sup>

The minimum performance specifications for GPWS provide alerting thresholds for the system based on the observable barometric and radar altitudes.<sup>13</sup> The minimum specifications only require a single alert. In practice, however, GPWS systems use a two-stage method of a caution (aural alerts of “sink rate” or “terrain”) followed by a warning (aural alert of “pull up”) if the terrain threat continues to grow.

Figure 1 shows an example alerting threshold diagram from the Boeing B-767 GPWS “excessive barometric descent rate” mode.<sup>14</sup> An aircraft that is descending at a constant 4000 ft/min, for example, generates a “sink rate” caution at an altitude of approximately 2000 ft above the terrain, and a “pull up” warning at an altitude of approximately 1200 ft above the terrain. Whether this warning provides enough time to avoid a CFIT accident depends on the pilot’s response latency, the aggressiveness with which the aircraft is pitched up, and on the rate at which the terrain gains higher altitudes.

An important consideration of GPWS design is the ability to predict how the placement of these alerting thresholds translates into safety improvements. To be accepted, an alerting system design must provide a desired level of safety improvement while not issuing an excessive number of nuisance alerts. One means of obtaining safety and false alarm performance measures is through exposing the system to specific situations that will be expected in operation. Several areas are known to be problematic for GPWS, for example. Approaches to runways at San Francisco, Pittsburgh, and Cincinnati, among others, have been observed to produce sudden changes in radio altitude measurements that can trigger false alarms.<sup>15</sup> Any newly developed systems or modifications to existing systems would need to be tested in these known problem areas to ensure that GPWS operates acceptably.

It is also desirable to expose the system to a wider variety of conditions than are possible by examining specific situations alone. To obtain a broad data set, it may be more straightforward to develop an analytical model of terrain and gather statistical predictions of performance than to run the system against a large number of actual terrain fields. The impact of uncertainties in vehicle state (position, velocity, etc.), sensor errors, and human performance can also typically be injected into the analytical model. Use of the statistical results, however, must be weighed against the assumptions behind the model, including the assumed probability of exposure to different types of terrain. Thus, statistical data provide a complementary view of system performance to site-specific observations.

### III. Terrain Profile Model

To probabilistically examine the effectiveness of GPWS in different types of terrain first requires a statistical model of the variations in terrain altitude. Some means of calculating the probability that the terrain takes on certain shapes is required. The probability that a collision will occur then depends on the probability that a terrain profile will exist that intersects the future trajectory of the aircraft.

There are several options for how to model a terrain field, as demonstrated in previous efforts evaluating TRN systems. One approach, for example, was to iteratively subdivide a region into squares while setting the altitude in each square according to a Gaussian distribution.<sup>10</sup> This provided a reasonable terrain field against which a TRN filter could be operated, but was not necessarily intended to statistically match terrain. Other methods rely on developing a stochastic process model of terrain, using parameters

such as correlation distance and slope variance to simulate different terrain roughness.<sup>5,9,16–18</sup>

In the present study of GPWS performance, a first-order Gauss–Markov model was developed to describe the statistics of terrain. A Markov chain was then used to calculate a probabilistic distribution of terrain altitude as a function of distance ahead of the aircraft. In this analysis terrain is treated as a stochastic first-order Markov process for several reasons. First, Markov models can often be used to describe natural processes; they therefore are likely to also describe the statistics of terrain.<sup>19</sup> Second, Markov processes are simple to define and manipulate using probability theory, which is a necessary step when predicting system performance. Obtaining the Markov model involves representing terrain altitude as a stochastic process, from which statistics can be measured and used to create simulated terrain fields. This requires first obtaining an empirical autocorrelation function of terrain profiles and then approximating this function using a curve fit with an ideal Markov process. Empirical collection of autocorrelation functions has been performed in prior work (e.g., see Ref. 17), but in the present work the approach is extended to a wider range of terrain types and is linked directly to a Gauss–Markov process. This facilitates the probabilistic computations discussed in the next section.

The autocorrelation function describes the statistical correlation between two samples of a signal taken a lag time  $\tau$  apart.<sup>19,20</sup> The autocorrelation function  $\phi_{yy}(\tau)$  for a continuous-time, stationary, ergodic function  $y(t)$  is defined by

$$\phi_{yy}(\tau) = \int_{-\infty}^{\infty} y(t)y(t + \tau) d\tau \quad (1)$$

If  $y(t)$  is a first-order Gauss–Markov process, Eq. (1) reduces to an even exponential function:

$$\phi_{yy}(\tau) = \sigma^2 e^{-|\tau|/\tau_0} \quad (2)$$

That is, the correlation between two samples of the process decreases exponentially as the lag time between samples increases. The parameters  $\sigma^2$  and  $\tau_0$  reflect the variance and length scale, respectively, of the fluctuations in the process. Equation (2) is sometimes written instead in terms of  $\beta = 1/\tau_0$ .

Consider now a discrete-time Markov process that has taken values  $y_0, y_1, y_2, \dots, y_{n-1}, y_n$  up to the present time  $n$ . A convenient property of first-order Markov processes is that the probability of the next value in the sequence  $y_{n+1}$  depends only upon the most recent value  $y_n$ . Then, a representative signal can be constructed without carrying along a complete history of all previous values in the signal. In fact, a discrete-time Markov process can be generated by the following system equation<sup>20</sup>:

$$y_{n+1} = e^{-\beta} y_n + \xi_n \quad (3)$$

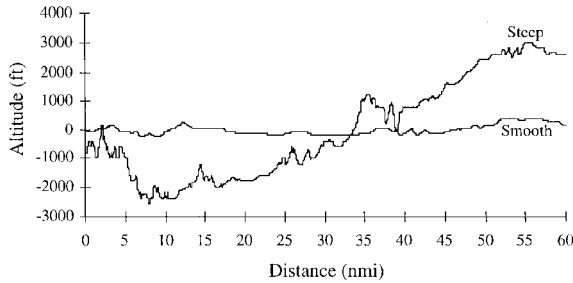
This process is termed a Gauss–Markov process when  $\xi_n$  is a zero-mean normally distributed random variable with variance  $\sigma^2(1 - e^{-2\beta})$ .

A large ensemble of actual terrain data was used to derive the statistics of this process. The terrain profile data were obtained from 1-deg digital elevation models (DEM) distributed by the U.S. Geological Survey, produced by the National Imagery and Mapping Agency from cartographic and photographic sources. The data used here covered the U.S. Great Plains and Rocky Mountain region in  $1 \times 1$  deg blocks between 102–112 deg West longitude and 32–49 deg North latitude. Ground elevation data are stored in the database every 3 arc seconds (approximately 100 m or 300 ft), with a vertical resolution of 1 m (3.3 ft). The accuracy of the database depends on the type of terrain being modeled, but is specified to have an absolute horizontal error (from a given feature to a datum location) less than 130 m (425 ft) at the 90% confidence level and an absolute vertical error (from a given feature to mean sea level) less than 30 m (98.5 ft) at the 90% confidence level.<sup>21</sup> Examples of two terrain profiles from the DEM database are shown in Fig. 2.

Because the statistics of terrain in a flat region are not the same as those for a mountainous region, the terrain profiles were separated

**Table 1 Terrain categories**

Terrain category	Altitude standard deviation, m	99% confidence interval (altitude span over 60 n miles)	Number of samples in database
Smooth	<84	<500 m	2651
Moderately smooth	84–167	500–1000 m	1996
Moderate	167–250	1000–1500 m	1432
Moderately steep	250–333	1500–2000 m	1018
Steep	>333	>2000 m	1353

**Fig. 2 Example true terrain samples (shifted vertically to have zero mean).**

into five categories based upon the variance of terrain altitudes in the sample, shown in Table 1. Given the altitude standard deviations shown in Table 1, 99% ( $\pm 3\sigma$ ) confidence intervals for terrain altitude range in each sample can be approximated and are also shown. For example, terrain in the moderate category would be expected to vary between 1000–1500 m in altitude over a distance of 60 n miles.

A total of 8450 terrain samples were taken from the database. Each sample was a North–South profile 1 deg long in latitude (60 n miles). Separate samples were taken every 72 arc seconds in longitude (approximately 1 n miles). Because each sample was 1 deg in length with data point spacing every 3 arc seconds, 1200 data points were available per terrain profile.

These samples were classified into one of the five terrain categories, and the empirical autocorrelation function  $\phi_{yy}(\tau)$  of the signal was calculated using

$$\phi_{yy}(\tau) = \frac{1}{T - \tau} \sum_{t=0}^{T-\tau} y(t)y(t + \tau) \quad (4)$$

where  $T$  is the total length of the record (1200 data points) and  $\tau$  is the lag between data points in the sample. The values of  $\phi_{yy}(\tau)$  were then averaged across the set of samples in the same altitude category to arrive at a representative autocorrelation function.

The autocorrelation function of an infinite-length single-order Markov process is exponential, as was shown in Eq. (2). When a finite-length sample is taken from a Markov process using Eq. (4), however, the resulting empirically determined autocorrelation function is not exponential.<sup>19,22</sup> The expected value of  $\phi_{yy}(\tau)$  for a finite-length record is given by

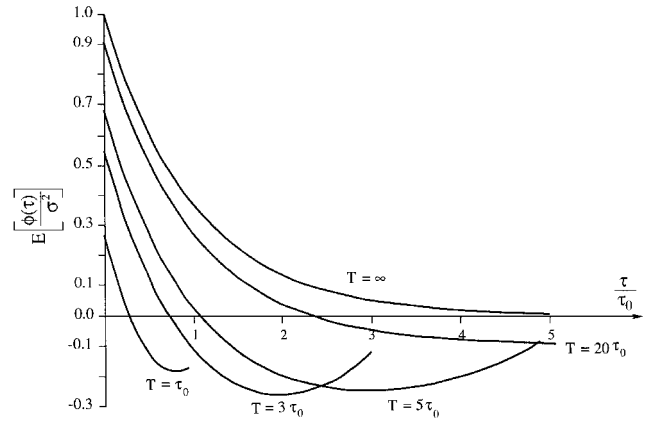
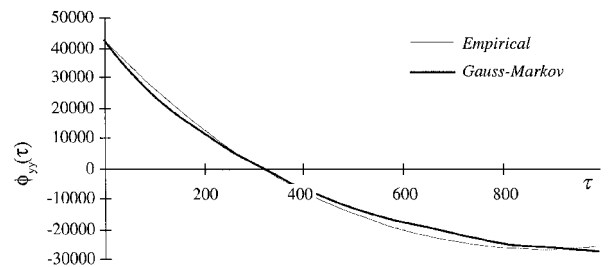
$$E[\phi_{yy}(\tau)] = \sigma^2 e^{-\tau/\tau_0} + \frac{2\sigma^2 \tau_0^2}{T^2} \left[ \frac{T}{\tau_0} - (1 - e^{-T/\tau_0}) \right] - \frac{4\sigma^2 \tau_0^2}{T(T - \tau)} \left\{ \frac{T - \tau}{\tau_0} - [1 - e^{-(T-\tau)/\tau_0}] \right\} - \frac{2\sigma^2 \tau_0^2}{T(T - \tau)} [1 - e^{-\tau/\tau_0} + e^{-T/\tau_0} - e^{-(T-\tau)/\tau_0}] \quad (5)$$

where  $\tau_0$  is the correlation time constant of the finite-length signal.<sup>22</sup> As shown in Fig. 3, as the record length increases relative to the correlation time constant the empirical autocorrelation function more closely approaches the ideal exponential function.

To develop an approximate fit to the empirically determined autocorrelation functions, Eq. (5) was first solved for  $\tau_0$  such that the zero-crossing point of the curve fit matched that of the empirical autocorrelation function. Then,  $\sigma$  was chosen such that the value

**Table 2 Fitted autocorrelation function parameters [Eq. (5)]**

Terrain category	$\sigma$ , m	$\tau_0$	$\beta$
Smooth	79	458	$2.2 \times 10^{-3}$
Moderately smooth	269	1551	$6.4 \times 10^{-4}$
Moderate	342	773	$1.3 \times 10^{-3}$
Moderately steep	415	492	$2.0 \times 10^{-3}$
Steep	1007	1633	$6.1 \times 10^{-4}$

**Fig. 3 Expected value of autocorrelation function for finite-length sample.<sup>22</sup>****Fig. 4 Empirical and fitted autocorrelation functions.**

of  $\phi_{yy}(0)$  for the fitted Markov process equaled that obtained empirically. This correction for a finite sample size was not applied in some prior work. Instead of fitting data using Eq. (5), Ref. 17 for example used the sum of two exponential functions to fit the data. This results in different correlation distances because the underlying models are different.

An example empirical autocorrelation function and a fitted Markov function [using Eq. (5)] is shown for the moderate terrain category in Fig. 4. The relatively close curve fit demonstrates that the Markov model is appropriate for capturing the statistical properties of terrain. Similar qualities of curve fits were obtained with the other terrain categories.

Table 2 shows the function parameters for the fitted autocorrelation function for each terrain category. The values for  $\sigma$  increase as the terrain categories change from smooth to steep. However,  $\tau_0$  does not show much correlation with the terrain category. Because the categories were defined based on variance, it is expected that  $\sigma$  should be different in each category. It appears, however, that the correlation distance for terrain is not strongly coupled with variance; smooth regions may have similar correlation distances to steep regions. This is in contrast to another terrain model in which correlation distance gradually increased with terrain roughness (Ref. 5), but is consistent with Ref. 17 where empirically determined correlation distances were found to have little relationship to terrain variance.

As a demonstration that the Markov modeling process just described is reasonable for terrain, comparisons of true terrain profiles against terrain generated using a Gauss–Markov process are shown in Fig. 5. The top plot shows a randomly selected smooth category

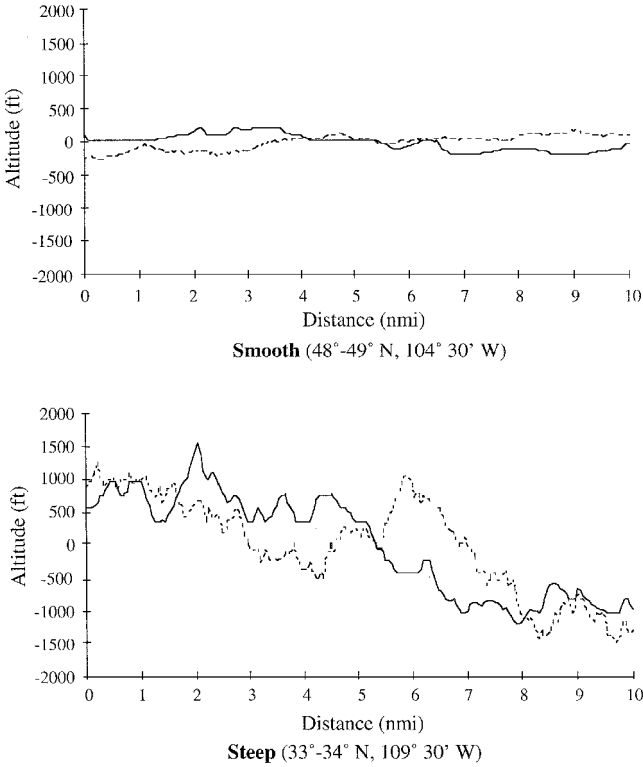


Fig. 5 Example terrain profiles (—, true terrain profile; ---, random Gauss-Markov sample. Samples shifted to zero mean).

terrain profile from the DEM database and a randomly generated Gauss-Markov profile using Eq. (3). The bottom plot shows randomly selected and randomly generated profiles from the steep terrain category. The Gauss-Markov model appears to represent the large-scale changes in terrain altitude well, and thus appears to be a reasonable method by which terrain may be handled probabilistically and compactly.

#### IV. Markov Chain

Having found the parameters needed to describe and generate terrain profiles using a Markov process, it is now possible to construct a Markov chain.<sup>25</sup> The purpose of the chain is to compute the probability that the altitude of terrain will exceed the aircraft's altitude along a given flight path. This then gives the probability that a CFIT accident occurs.

Given a discrete-time Markov process, a set of discrete states can be constructed that describe the possible values that the process may take. In this case these states correspond to different terrain altitude bins. At each time step there is a certain probability that the state of the process will change from its current value  $y_n$  to some new value  $y_{n+1}$ . In Fig. 6 a five-state Markov chain is shown, with the transition probability  $p_{ji}(n)$  defined as the probability that the process will change from state  $y_n = i$  to state  $y_{n+1} = j$ .

Next, a state vector  $y_n$  is defined, which holds the probabilities that the process takes on the value of each state in the chain at time step  $n$ :

$$y_n = \begin{bmatrix} \text{probability that altitude is in state 0 at time step } n \\ \vdots \\ \text{probability that altitude is in state } m \text{ at time step } n \end{bmatrix} \quad (6)$$

The transition probabilities can also be placed into a state transformation matrix:

$$T_n = \begin{bmatrix} p_{11}(n) & p_{12}(n) & \cdots & p_{1m}(n) \\ p_{21}(n) & p_{22}(n) & \cdots & p_{2m}(n) \\ \vdots & \vdots & \ddots & \vdots \\ p_{m1}(n) & p_{m2}(n) & \cdots & p_{mm}(n) \end{bmatrix} \quad (7)$$

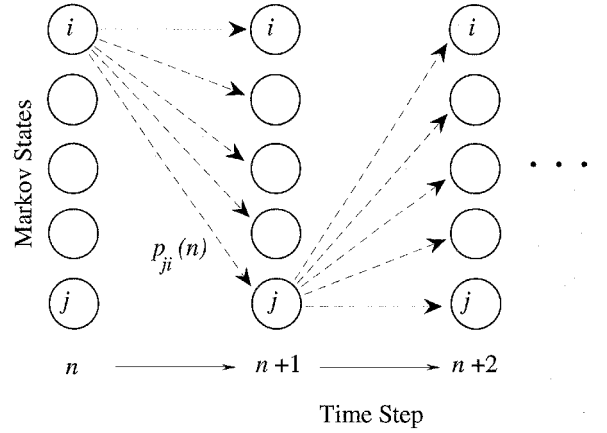


Fig. 6 Markov chain model.

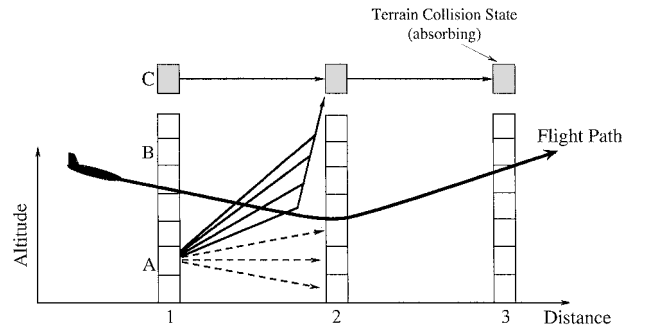


Fig. 7 Markov chain propagation method.

Where  $p_{ji}(n)$  is the probability that the state changes from  $i$  to  $j$  at time step  $n$ .

Given an initial state probability vector  $y_0$ , the probabilities of the process being in each state after one time step are given by

$$y_1 = T_0 y_0 \quad (8)$$

By extension the probabilities of the process taking on each state at time step  $n$  are then given by

$$y_n = T_{n-1} T_{n-2} \cdots T_0 y_0 \quad (9)$$

Thus, by concatenating the transformation matrices together, the probability that the process takes on a certain value at a future time step can be calculated.

The procedure for using the Markov chain involves tracking the probability that the terrain reaches different altitudes as the aircraft flies along. Starting with an initial AGL altitude, the probability that the terrain is at a given altitude as the aircraft flies along is calculated. This involves using the state transition matrix just described. Any terrain altitudes above the aircraft's flight path represent cases in which an impact occurs. Each state which is above the aircraft's altitude is tagged and immediately transitions to an absorbing terrain collision state. For example, in Fig. 7 a hypothetical aircraft flight path is shown relative to the Markov chain. Consider the case in which terrain altitude is in state A at the first time step. The state transitions shown with the dashed arrows represent potential future terrain altitudes below the aircraft. However, any transition from A to a state above the aircraft's flight path will result in a collision; the probabilities of these transitions are combined into a transition into the terrain collision state (shown by the solid arrow). Similarly, terrain currently above the aircraft (B) or in a terrain collision state (C) will transition directly to the next terrain collision state. Thus, the probability that terrain is in the terrain collision state at each step in the process represents the running probability that a collision with terrain has occurred.

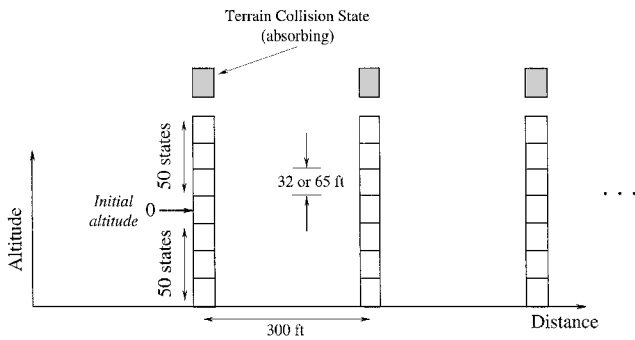


Fig. 8 Markov chain schematic.

Each distance step (points 1, 2, and 3 in Fig. 7) corresponds to one data point interval from the terrain database, equivalent to 3 arc seconds (or 300 ft). A total of 50 state bins were provided above the initial terrain altitude, each with a height of 10 to 20 m (32 to 65 ft) depending on the type of terrain under study. Because terrain altitude can drop and then rise, an additional 50 state bins were also used below the initial terrain altitude. Also, a terrain collision state was created and used to store those cases in which terrain altitude had risen above the aircraft's altitude. This collision state was absorbing: once entered, the process would remain in that state. A schematic of the Markov chain is shown in Fig. 8.

The probability that the process transitions from a starting altitude bin at step  $n$ ,  $y_n$ , to an altitude bin at step  $n + 1$ ,  $y_{n+1}$ , can be found from the process defined by Eq. (3). The transition probability aggregated over a state bin with height  $h$  is given by

$$p_{y_{n+1}, y_n}(n) = \int_{y_{n+1}-h/2}^{y_{n+1}+h/2} \frac{1}{\sqrt{2\pi\sigma^2(1-e^{-2\beta})}} \times \exp\left[-(y - e^{-\beta}y_n)^2 / 2\sigma^2(1-e^{-2\beta})\right] dy \quad (10)$$

where  $\sigma$  and  $\beta$  are the autocorrelation function parameters from Table 2.

Equation (10) was used to construct a complete state transition matrix for a given terrain category. Next, the aircraft's flight path was superimposed over the Markov chain. Those states above the aircraft's altitude resulted in a modification to the transition matrix such that there would be a direct transition to the absorbing state. The probabilities corresponding to transitions to states above the aircraft's altitude (e.g., the solid transition lines in Fig. 7) were summed and became the probability corresponding to a transition to the absorbing state. As the aircraft changes altitude, a new  $T$  matrix needs to be defined, taking into account the new impact states.

## V. Example Performance Evaluation During Descent

The performance of GPWS was evaluated for a range of descent rates and terrain types. To simplify the discussion, only the smooth, moderate, and steep terrain categories are considered here.

As a baseline, it is assumed that when a "pull up" warning is issued a standard maneuver of a 5-s delay followed by a 2 deg/s pull up to a 15-deg flight-path angle is used. This maneuver corresponds to typical response times and the suggested flight-path angle rate when a GPWS alert is issued.<sup>24,25</sup> A 5-s response time delay is also assumed in other alerting systems such as the Traffic Alert and Collision Avoidance System.<sup>26</sup> A flight path for this maneuver was then computed using a point-mass model of an aircraft flying at a constant speed of 170 kn. This speed is consistent with a jet transport flying an approach segment, though other speeds could be tested. The probability of colliding with terrain following an alert  $P(C)$  was then computed using the Markov chain already described.

Contours of constant  $P(C)$  are shown in Fig. 9 as a function of altitude and descent rate at the moment that a hypothetical GPWS warning was generated. Also shown for reference in Fig. 9 are the actual B-767 GPWS alerting thresholds.

From Fig. 9 it can be seen that the GPWS warning thresholds provide for a very low (less than  $1 \times 10^{-8}$ ) probability of collision for

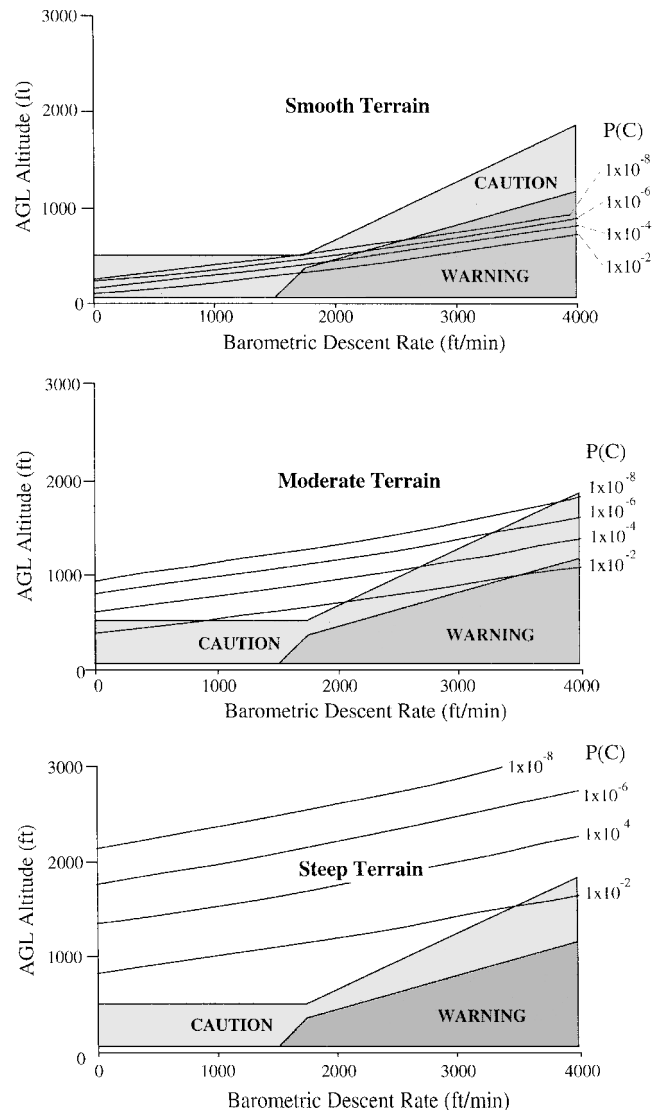


Fig. 9 Comparison of GPWS thresholds and probability of collision  $P(C)$ .

smooth terrain when an alert is issued at large descent rates. Lower descent rates actually incur a higher probability of collision because alerts are delayed until the aircraft is quite close to the ground. In the moderate and steep terrain categories GPWS cannot provide as high a degree of protection, with probabilities exceeding 0.01. If the alerting thresholds were expanded to compensate, however, an increased rate of nuisance alarms would likely occur. The decreased performance of GPWS in steep terrain is a symptom of the fact that the terrain ahead of the aircraft is unobservable to the alerting system.

### A. Safety/Nuisance Alert Tradeoff

Next, the degree to which nuisance alarms and safety can be traded off against one another in the placement of the alerting thresholds is described. The methodology used here is based on that presented in Ref. 27.

The preceding section provided a method to compute the probability of a collision once an alert is issued  $P(C)$ , assuming a given avoidance maneuver was followed. This is a measure of the level of safety provided by GPWS. Alternatively, the probability of successful alert  $P(SA)$  can be defined as

$$P(SA) = 1 - P(C) \quad (11)$$

Therefore,  $P(SA)$  is a measure of the degree of success of GPWS in preventing a collision.

A second metric, the probability that a GPWS alert is unnecessary  $P(UA)$ , is also required to quantitatively describe the performance tradeoffs involved in the alerting threshold placement.  $P(UA)$  is generally a difficult metric to define because the concept of an unnecessary alert is somewhat subjective and situation dependent. To provide a consistent and representative measure here, however, an alert is considered to be unnecessary if the aircraft would not collide with terrain within 3 n miles along its current descent path. The use of 3 n miles as a limit is representative of the length scale over which a typical terrain proximity incident occurs and so serves as a surrogate for the need to issue a GPWS alert. This distance also corresponds to the maximum advance warning time typically used in GPWS systems (approximately 60 s at a speed of 170 kn).<sup>28</sup> The following analysis could be repeated with other definitions, if desired.  $P(UA)$  is then given by

$$P(UA) = 1 - P(\text{collision within 3 n miles along current descent path}) \quad (12)$$

The probabilities of a collision were then computed for 1) the case in which an alert is issued [yielding  $P(SA)$ ] and 2) the case in which the aircraft continues along its current descent path for 3 n miles [yielding  $P(UA)$ ]. This computation was performed using the Markov chain just described, with the two different aircraft flight paths as shown in Fig. 10. The simulation was repeated at varying AGL altitudes and descent rates to explore the level of safety and probability of unnecessary alert for a range of potential GPWS alerting thresholds.

**B. Results**

One example evaluation is presented here for an aircraft at 170 kn with a descent rate of 3000 ft/min. The results are plotted as  $P(SA)$  vs  $P(UA)$ , resulting in system operating characteristic (SOC) curves.<sup>27</sup> SOC curves show the possible operating conditions for GPWS as a function of the placement of the alerting threshold. A given threshold setting (i.e., alerting with a given projected time to impact) results in operating at a specific point in the  $P(SA)$ ,  $P(UA)$  plane. Varying the threshold setting traces out an SOC curve.

Two SOC curves are shown in Fig. 11: one for the operation of GPWS over smooth terrain and one for operation over steep terrain. For clarity, the horizontal scale has been changed to focus on the region where  $P(UA) < 0.10$ . The smooth terrain SOC curve goes up the left axis, passes very close to the ideal operating point of  $P(UA) = 0$ ,  $P(SA) = 1$ , and then continues along the top of the plot to the point  $P(UA) = 1$ ,  $P(SA) = 1$ . The steep terrain SOC bends away from the upper-left corner, indicating that GPWS cannot provide a high safety level [ $P(SA)$ ] in steep terrain without incurring nuisance alerts.

For reference, the operating point of the actual B-767 GPWS alerting threshold is shown in Fig. 11 by a small circle on each SOC curve. The SOC curve then shows that if the alerting threshold were made to be more conservative (that is, to alert at a higher altitude given the descent rate), then the probability of a successful alert would increase, but at the expense of rapidly increasing the probability of unnecessary alert over steep terrain. Also, Fig. 11 illustrates that GPWS is able to operate at a higher  $P(SA)$  and a lower  $P(UA)$  in smooth terrain than in steep terrain. This is because

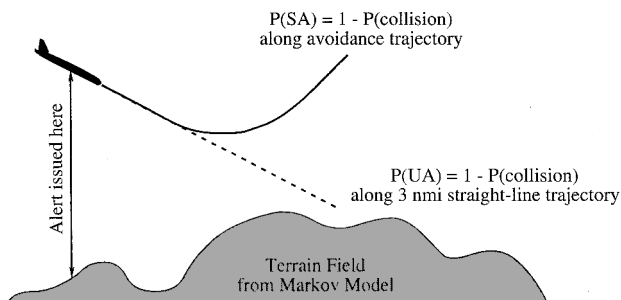


**Fig. 10** Trajectories used to compute  $P(SA)$  and  $P(UA)$ .

**Table 3** Summary of B-767 GPWS performance at 3000 ft/min descent rate (excessive descent rate mode)

Terrain category	$P(UA)$	$P(C)$
Smooth	$1 \times 10^{-4}$	$< 1 \times 10^{-8}$
Steep	0.08	0.03

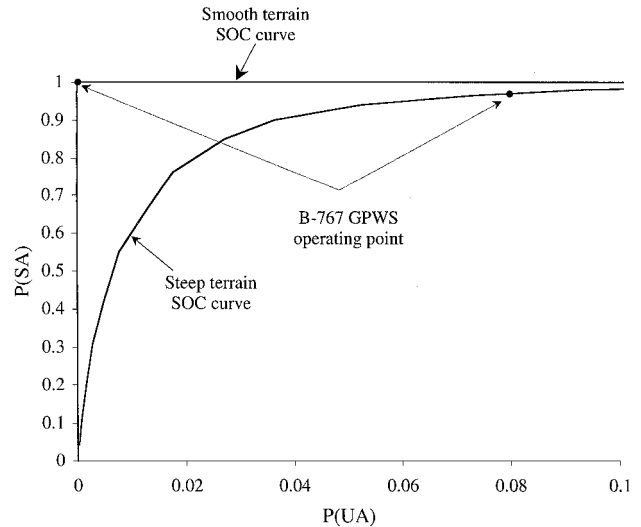


**Fig. 11** SOC curves (3000 ft/min descent rate at 170 kn).

of the reduced uncertainty in the smooth terrain case regarding the terrain altitudes ahead of the aircraft. Similar SOC curves can be generated for the other terrain categories and for varying speeds and descent rates.

As summarized in Table 3, the probability that a B-767 GPWS alert is unnecessary increases from  $1 \times 10^{-4}$  to 0.08 between the smooth and steep terrain categories. The probability that a collision occurs when a GPWS alert is issued [ $1 - P(SA)$ ] increases from  $< 1 \times 10^{-8}$  to 0.03 between the same terrain categories. Thus, there is a decrease in performance both in terms of increased nuisance alarms and late alerts when over steep terrain. Without additional and higher-quality information regarding the terrain ahead of the aircraft, GPWS cannot perform any better than the SOC curve shows. However, given these constraints on GPWS, it appears from the SOC curve that the B-767 alerting thresholds are set at a reasonable location to balance safety against nuisance alarms.

This type of analysis can also be extended to examine the impact of changes in the avoidance trajectory on the performance of the alerting system. A shorter response latency or more aggressive pull-up maneuver could improve the safety of the alerting system. The assumption in Fig. 11 was that there was a 5-s pilot response delay. It is interesting, however, to observe the potential benefit that a faster response time could have on GPWS operation. Accordingly, the preceding analysis was repeated for the case in which the response delay was 2 s instead of 5 s. Also, the aggressiveness of the pull-up maneuver can be varied and observed using SOC curves. Increasing the pitch rate or load factor during the pull-up and so improves the probability of escaping from the terrain.

Figure 12 shows an SOC plot for steep terrain under three different pull-up conditions: (solid line) the baseline case (repeated from Fig. 11) with a response delay of 5 s and pitching at 2 deg/s (a load factor of 1.3 g), (long dashed line) a reduced delay of only 2 s and pitching at 2 deg/s (1.3 g), and (short dashed line) a response delay of 5 s but more aggressive pull-up at 3.25 deg/s (a load factor of 1.5 g). The effect of a higher load factor during the pull-up is similar to reducing the response latency: a higher level of  $P(SA)$  and lower value of  $P(UA)$  is possible in the more aggressive cases. At the B-767 GPWS threshold setting [where  $P(UA) = 0.08$ ], decreasing response time to 2 s would increase  $P(SA)$  from 0.97 to 0.994.

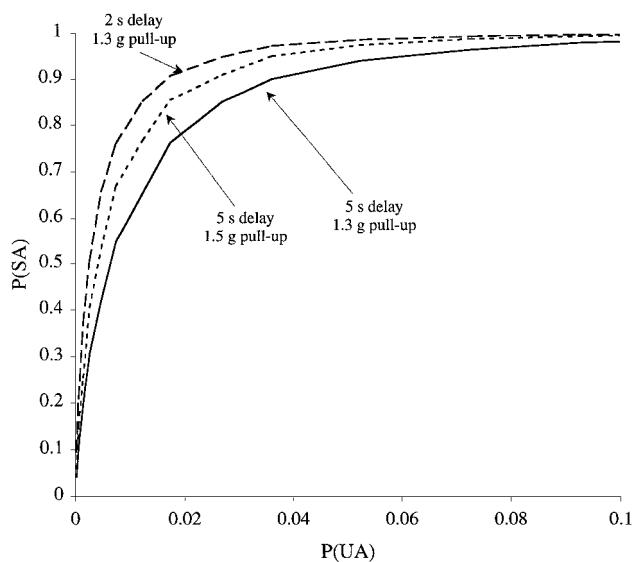


Fig. 12 Effect of pull-up trajectory on SOC curves (steep terrain, 3000 ft/min descent rate at 170 kn).

Alternatively, increasing the pull-up load factor to 1.5 g would increase  $P(SA)$  from 0.97 to 0.990. In this manner the analysis can be used to quantitatively compare changes in not only alerting thresholds, but also in pilot response time or pull-up load factor.

## VI. Concluding Remarks

This paper has four objectives: first, to present a statistical terrain model for analyses of terrain referenced navigation, terrain following, or terrain avoidance system performance; second, to outline a general process by which alerting system thresholds can be evaluated; third, to provide specific performance results for a case study of the B-767 GPWS; and fourth, to show how modifications in GPWS alerting threshold settings would translate into changes in safety or false alarm probability.

Alerting systems are used so that safety, on average, can be improved. To be accepted, new alerting systems must demonstrate this safety enhancement but also must not issue an excessive rate of nuisance alarms. Observation of system performance in specific, known problem areas can be beneficial in this regard to highlight any necessary modifications in design. It is also likely that a broader statistical estimate of performance over a range of conditions would be useful in determining whether or how to modify the design of an alerting system. This paper presents such a statistical analysis of GPWS. In addition to providing a point solution for false alarm probability and safety in a given case study, the method presented here also draws performance tradeoff curves that aid in determining whether simple changes in threshold settings would be beneficial, or if higher-quality sensor information is needed to enable improved performance.

A Gauss–Markov process was used to create an analytical model of terrain to estimate the probability of terrain impact following a GPWS alert. The Markov model allows for a compact representation, requiring only two parameters to define a terrain profile, and is well-suited for probabilistic analyses using a Markov chain. The model parameters were set such that the autocorrelation of the model process matched the autocorrelation of an ensemble of actual terrain profiles from a database. As an analytical tool, the Gauss–Markov process presented here could also be used in other applications such as evaluation of terrain-following or TRN algorithms.

The stochastic terrain profile was compared to the flight trajectory of an aircraft performing a 1.3-g load factor pull-up maneuver following a 5-s delay from a GPWS alert. Using the terrain model in an example high-descent rate case, GPWS is shown to provide a significantly higher safety level when an alert is issued over relatively smooth terrain compared against steep terrain. Probability of terrain collision following an alert was less than  $10^{-8}$  for smooth terrain and approximately 0.03 over steep terrain. The probability that an

alert would be a false alarm also increases over steep terrain (0.08) compared to smooth terrain ( $10^{-4}$ ). From the performance tradeoff curves that were also generated, it can be seen that safety level in steep terrain can only be increased while also greatly increasing false alarm probability. Performance of GPWS with a shorter response time delay or a more aggressive pull-up maneuver is also presented. Reducing the response time to 2 s or increasing the pull-up load factor to 1.5 g reduces the probability of collision following an alert from 0.03 to approximately 0.01 over steep terrain. These analyses quantitatively show the limitations of GPWS that occur because information about terrain ahead of the aircraft is unavailable to the system. The higher uncertainty in ground altitude in a steep terrain region translates into a poorer design tradeoff in which either safety or false alarm rate must be sacrificed.

Certainly, performance measures must also be collected through actual field trials. Indeed, GPWS has been modified in the past in response to observed performance on aircraft. Still, during initial development statistical analyses as outlined here could have significant benefit in selecting an appropriate design condition. Performance tradeoff curves can also have value in determining how a design might be modified to improve its acceptability even after it is fielded.

## References

- <sup>1</sup>National Transportation Safety Board, "Aircraft Accident Report—Trans World Airlines, Inc. Boeing 727-231, N54328, Berryville, Virginia, December 1, 1974," Rept. NTSB-AAR-75-16, Washington, DC, 26, Nov. 1975.
- <sup>2</sup>Federal Aviation Administration, *U.S. Federal Aviation Regulations (FAR)*, §121.360, Washington, DC, 1999.
- <sup>3</sup>Bateman, D., "How to Terrain-Proof Corporate and Regional Aircraft," *Flight Safety Digest*, Vol. 12, No. 8, 1993, pp. 38–67.
- <sup>4</sup>DeCelles, J. L., "The Delayed GPWS Response Syndrome," *Air Line Pilot*, Vol. 61, No. 1, 1992, pp. 26–29, 54.
- <sup>5</sup>Baird, C. A., Collins, N., and Drew, M., "Terrain-Aided Navigation and Target Acquisition on the AFTI/F-16," *Advances in Techniques and Technologies for Air Vehicle Navigation and Guidance*, CP-455, AGARD, 1989, pp. 62-1–62-12.
- <sup>6</sup>Grey, D. M., and Dale, R. S., "Recent Developments in TERPROM," *Advances in Techniques and Technologies for Air Vehicle Navigation and Guidance*, CP-455, AGARD, 1989, pp. 12-1–12-15.
- <sup>7</sup>Bennett, P. J., "The Use of Digital Map Data to Provide Enhanced Navigation and Displays for Poor Weather Penetration and Recovery," *Journal of Navigation*, Vol. 46, No. 2, 1993, pp. 208–222.
- <sup>8</sup>Hewitt, C., and Broatch, S. A., "A Tactical Navigation and Routing System for Low-Level Flight," *Low-Level and Map-of-the-Earth Night Operations*, CP-563, AGARD, 1995, pp. 11-1–11-10.
- <sup>9</sup>Zelenka, R. E., Yee, Z., and Zirkler, A., "Flight Test of Radar Altimeter Enhancement for Terrain-Referenced Guidance," *Journal of Guidance, Control, and Dynamics*, Vol. 18, No. 4, 1995, pp. 702–708.
- <sup>10</sup>Enns, R., and Morrell, D., "Terrain-Aided Navigation Using the Viterbi Algorithm," *Journal of Guidance, Control, and Dynamics*, Vol. 18, No. 6, 1995, pp. 1444–1449.
- <sup>11</sup>Kuchar, J. K., and Hansman, R. J., "Part-Task Simulator Evaluations of Advanced Terrain Displays," Society of Automotive Engineers, SAE-9932570, Sept. 1993.
- <sup>12</sup>AlliedSignal Aerospace, "Enhanced Ground Proximity Warning System Product Description," AlliedSignal, Redmond, WA, 13 May 1996.
- <sup>13</sup>Radio Technical Committee on Aeronautics (RTCA), "Minimum Performance Standards—Airborne Ground Proximity Warning Equipment," Document RTCA/DO-161A, Washington, DC, 27 May 1976.
- <sup>14</sup>Boeing Commercial Airplane Co., "Boeing 767 Operations Manual," Boeing Document No. D632T001-200, Seattle, WA, 25 July 1983.
- <sup>15</sup>Pritchett, A. R., "Reviewing the Role of Cockpit Alerting Systems," *Human Factors in Aerospace Safety*, Vol. 1, No. 1, 2001, pp. 5–38.
- <sup>16</sup>Tonkin, S. P., and Wood, M. A., "Stochastic Model of Terrain Effects upon the Performance of Land-Based Radars," *Target and Clutter Scattering and Their Effects on Military Radar Performance*, CP-501, AGARD, 1991, pp. 32-1–32-9.
- <sup>17</sup>Carlson, G. E., and Bair, G. L., "Simple Generation of One-Parameter Pseudoterrain Surfaces," *IEEE Transactions on Aerospace and Electronic Systems*, Vol. 5, No. 5, 1979, pp. 735–738.
- <sup>18</sup>Baird, C., "Design Techniques for Improved Map-Aided Navigation," *Proceedings of the IEEE National Aerospace and Electronic Conference*, Inst. of Electrical and Electronics Engineers, New York, 1985, pp. 231–238.
- <sup>19</sup>Gelb, A. (ed.), *Applied Optimal Estimation*, The Analytic Sciences Corp., Massachusetts Inst. of Technology Press, Cambridge, MA, 1974, pp. 86–90.
- <sup>20</sup>Brown, R. G., and Hwang, P. Y. C., *Introduction to Random Signals and Applied Kalman Filtering*, Wiley, New York, 1992, Chap. 2.

- <sup>21</sup>U. S. Geological Survey, "Data User Guide 5: Digital Elevation Models," Branch of Technical Standards and Product Development, Reston, VA, 1993.
- <sup>22</sup>Weinstock, H., "The Description of Stationary Random Rate Processes," Massachusetts Inst. of Technology Instrumentation Lab. Rept. E-1377, Cambridge, MA, 1 July 1963.
- <sup>23</sup>Kemeny, J. G., and Snell, J. L., *Finite Markov Chains*, D. Van Nostrand Co., Princeton, NJ, 1967, Chap. 3.
- <sup>24</sup>Poole, R. A., "Whoop Whoop Pull Up," *Flying Safety*, Vol. 48, No. 6, 1992, pp. 16, 17.
- <sup>25</sup>Lewis, C., "Whoop, Whoop, Pull Up!," *Flight Deck*, American Airlines

- Flight Dept. Flight Academy, Dallas, TX, Nov./Dec. 1994, pp. 7-13.
- <sup>26</sup>Radio Technical Committee on Aeronautics (RTCA), "Minimum Performance Specifications for TCAS Airborne Equipment," Document RTCA/DO-185, Washington, DC, Sept. 1983.
- <sup>27</sup>Kuchar, J. K., "Methodology for Alerting-System Performance Evaluation," *Journal of Guidance, Control, and Dynamics*, Vol. 19, No. 2, 1996, pp. 438-444.
- <sup>28</sup>Bateman, D., "Development of Ground Proximity Warning Systems (GPWS)," Royal Aeronautical Society Controlled Flight into Terrain One Day Conf., Royal Aeronautical Society, Nov. 1994, pp. 3.1-3.9.